Dynamic Stark effect and interference photoelectron spectra of H_2^+

Chuan Yu, Ning Fu, Tian Hu, Guizhong Zhang, and Jianquan Yao

College of Precision Instrument and Optoelectronics Engineering, Key Laboratory of Optoelectronic Information and Technology Science (Ministry of Education), Tianjin University, Tianjin 300072, People's Republic of China

(Received 2 September 2013; published 8 October 2013)

For atomic hydrogen, an interference structure has been theoretically found to appear in the photoelectron spectra induced by strong extreme ultraviolet (XUV) laser pulses [Demekhin and Cederbaum,Phys. Rev. Lett. **108**, 253001 (2012)]. For molecular hydrogen ion H_2^+, our present work provides the results of the numerical simulation on its photoelectron spectra in an XUV photoionization process. The interference feature in the photoelectron spectra is investigated with respect to the dynamic Stark effect and the XUV laser parameters. The research outcome is that our numerical findings corroborate the prediction for the emergence of the modulation structures in the photoelectron spectra, similar to those already found for a hydrogen atom. For an XUV laser pulse with photon energy well above the ionization threshold of H_2^+, the dynamic Stark effect is prominently demonstrated for certain values of laser parameters such as intensity and pulse duration. The deployed one-dimensional model and the plane-wave description for the continuum states for the molecular hydrogen ion are of crucial significance in modeling the molecular system. The numerical computation is made feasible by using a hybrid algorithm. We advocate an ensemble physical picture to decipher the physical mechanism for the formation of the interference photoelectron spectra by taking into account the nuclear degree of freedom. It is anticipated that more quantitative investigations on the Stark effect concealed in the photoelectron spectra created by single XUV photons are needed plus experimental verifications.

DOI: 10.1103/PhysRevA.88.043408 PACS number(s): 33.20.Rm, 82.50.Kx

I. INTRODUCTION

With the revolution of light sources from Ti:sapphire lasers to x-ray free-electron lasers [1–3], research on laser-matter interactions burgeons in both theoretical and experimental aspects, and experimental verifications of theoretical findings are becoming more and more feasible. An ultrashort laser pulse with unprecedented high carrier frequency can serve as an effective tool for probing and controlling the microprocess in atoms and molecules [4–6]. More importantly, the achievable intensity of the ultrashort laser pulses with single-photon energy well above the ionization threshold of many atoms and molecules stimulates deeper investigations of the single-photon excitation. For instance, studies on the dynamic or ac Stark effect [7–9] demonstrate unambiguously novel findings [10–12]. The helium atom was investigated for the ac Stark effect with a combined pulse train of near-infrared and extreme ultraviolet (XUV) pulses, and a subcycle energy-level shift was found [10]. For the hydrogen atom excited by a single XUV photon, Demekhin and Cederbaum [11] reported that the dynamic Stark effect induced the strong interference structures in the photoelectron spectra, which were also observed in the above-threshold ionization peaks [13,14]. In addition, they presented a transparent physical picture for the XUV laser ionization process by virtue of the rotating wave approximation (RWA) [15] and the local approximation [16,17], thus shedding light on the research context in the XUV excitation reign to come. As for multielectron atoms, a linear Stark effect for sulfur in the presence of a strong high-frequency laser field was observed theoretically for specific values of the laser parameters [12].

Inspired by pioneering work on atomic hydrogen [11], we envisage that the interference feature would equally appear in the photoelectron spectra of molecular systems. Unlike atoms, molecules inherently entangle the nuclear degree of freedom with the electronic degree of freedom, which poses a challenge to the available computing capability. For the hydrogen atom irradiated with intense XUV laser pulses, we have extended the studies to the plane-wave approximation for the continuum states and reduced the simulation to one dimension [18]. Now we further investigate the simplest molecule H_2^+, of which the final continuum states and the transition dipole moment are otherwise difficult to obtain. As will be explained later, the computation of the molecular photoelectron spectra requires numerically solving a series of the nuclear continuum-state wave functions and integrating them over the entire nuclear coordinate. The computing obstacles are overcome by using a one-dimensional (1D) model [19–21] for the molecule and a hybrid scheme [22,23] in the simulation. The computation speed is henceforth much boosted, enabling us to fulfill the numerical task.

Our work focuses on molecular hydrogen ion H_2^+ exposed to intense XUV laser pulses with varying pulse parameters. We report the interference feature in the photoelectron spectra of H_2^+ induced by the dynamic Stark effect of the nuclear ground state. Our research outcome manifests similar and distinct spectral characters as compared to atomic hydrogen. We also propose an approximation theory for the spectral characters in the molecular case, which indicates that a crucial factor contributing to the interference in the photoelectron spectra is the potential-energy surfaces (PESs) of the molecule. Specifically, the summation of the electronic wave packets dislodged at different internuclear separations smears the interference fringes in the photoelectron spectra, which demarcates molecules from atoms.

This paper is therefore organized as follows. In Sec. II we briefly describe the theoretical and numerical approaches to

 ©2013 American Physical Society

obtain the photoelectron spectra of H_2^+. Subsequently, the computed results are presented and discussed in Sec. III. Finally, we summarize our findings in Sec. IV.

II. THEORETICAL MODEL

We deploy the traditional 1D model for H_2^+ and an XUV laser field linearly polarized along the internuclear separation direction. The simplicity of this molecular workbench allows us to focus on the electronic transition from the ground state to the continuum states, since there is no other process necessary to consider. The photoelectron spectra are investigated by virtue of the customary Born-Oppenheimer approximation [24,25], which separates the nuclear and electronic degrees of freedom. As a consequence, the total wave function for H_2^+ can be composed of the linear combination of the products of the electronic and nuclear wave functions:

$$\Psi(R,x,t) = \psi_g(R,t)\chi_g(R,x) + \int d\varepsilon \widetilde{\psi}_\varepsilon(R,t)\chi_\varepsilon(R,x), \quad (1)$$

where $\chi_g(R,x)$ and $\chi_\varepsilon(R,x)$ are the electronic wave functions for its ground state and the continuum state of electron energy ε, and $\psi_g(R,t)$ and $\widetilde{\psi}_\varepsilon(R,t)$ are the corresponding nuclear wave functions.

Considering the dipole interaction with the laser field,

$$E_L(t) = E_0 g(t)\cos(\omega t) = E_0 \exp(-t^2/\tau^2)\cos(\omega t), \quad (2)$$

and redefining [26] $\psi_\varepsilon = \widetilde{\psi}_\varepsilon \exp(+i\omega t)$, we write the time-dependent Schrödinger equation [22] as the following set of equations under the RWA [atomic units (a.u.) are used]:

$$i\frac{\partial}{\partial t}\psi_g = \left[\frac{1}{2\mu}\frac{\partial^2}{\partial R^2} + V_g(R)\right]\psi_g + \int d\varepsilon \frac{1}{2} D_\varepsilon^*(R) E_0 g(t)\psi_\varepsilon, \quad (3a)$$

$$i\frac{\partial}{\partial t}\psi_\varepsilon = \left[\frac{1}{2\mu}\frac{\partial^2}{\partial R^2} + V_\varepsilon(R) - \omega\right]\psi_\varepsilon + \frac{1}{2} D_\varepsilon(R) E_0 g(t)\psi_g, \quad (3b)$$

where $\mu = 1836/2$ is the reduced nuclear mass and $D_\varepsilon(R) = \int dx\, \chi_\varepsilon^*(R,x) x \chi_g(R,x)$ is the dipole transition moment. $V_g(R)$ and $V_\varepsilon(R)$ are the potential-energy surfaces (PESs) [25] for the ground state and the continuum state of electron energy ε. Their detailed expressions adopted in our numerical simulation are as follows (the parameters are given in Ref. [27]):

$$V_g(R) = A\{\exp[-2\beta(R - R_e)] - 2\exp[-\beta(R - R_e)]\} + B, \quad (4a)$$

$$V_\varepsilon(R) = 1/R + \varepsilon. \quad (4b)$$

We evolve Eqs. (3) with the following initial conditions:

$$\psi_g(R,-\infty) = \psi_{g0}, \quad (5a)$$

$$\psi_\varepsilon(R,-\infty) = 0, \quad (5b)$$

where ψ_{g0} is the nuclear ground-state wave function computed by the imaginary time relaxation method [28].

In the traditional numerical algorithm for Eqs. (3), a matrix of huge dimension is mandatory for precision purposes, which will, however, pose a challenge for the quantum wave-packet calculation [22]. We surmount this obstacle by utilizing an efficient hybrid scheme [22,23] in simulating wave-packet dynamics, i.e., by treating the nuclear motion and the electron transition with separate algorithms alternatively. The dipole transition moment D_ε, which is essential to the simulation, is computed approximately by using the 1D plane wave for the electronic continuum-state wave function. An absorbing mask function [29] of the form $f(R) = 1/\{1 + \exp[\eta(R - R_{\rm abs})]\}$ is utilized at each temporal step on the nuclear wave functions to avoid unphysical reflections at the space grid boundary, albeit that the calculation details convince us that the absorbed wave function is quite trivial. All the computed results are checked for precision purposes by refining the grid size and density.

Finally, the intensity of the photoelectron spectrum at a given time is proportional to $\sigma(\varepsilon,t) = \int dR|\psi_\varepsilon(R,t)|^2$. The final spectrum at the end of the laser-molecule interaction process is proportional to $\sigma(\varepsilon,+\infty)$. It should be noted that the photoelectron spectrum corresponds to the detection in the direction of the laser polarization and the 1D model can be deployed for the linearly polarized laser only.

III. RESULTS AND DISCUSSION

In this section we show the results of our numerical simulation performed for an XUV laser pulse with carrier frequency $\omega = 60$ eV, the single-photon energy of which suffices to ionize the ground-state H_2^+. Figure 1 demonstrates the photoelectron spectra of H_2^+ under the excitation of the XUV laser field of pulse width $\tau = 8 * 2\pi/\omega = 0.547$ fs (corresponding to the full width at half maximum $2\sqrt{\ln 2}\tau = 0.911$ fs), while the peak intensity (defined as $E_0^2/8\pi\alpha$ with α being the fine-structure constant) is changed over a large range. One can see the existence of modulation structures in the photoelectron spectra, which is similar to that of a hydrogen atom [11]. It is also discernible that (i) the spectral peaks are located at an energy higher than the single-photon energy (60 eV) minus the ionization potential at the equilibrium internuclear separation $R_e = 2$ a.u. (approximately 30 eV); (ii) the peaks shift to higher energy positions with increasing

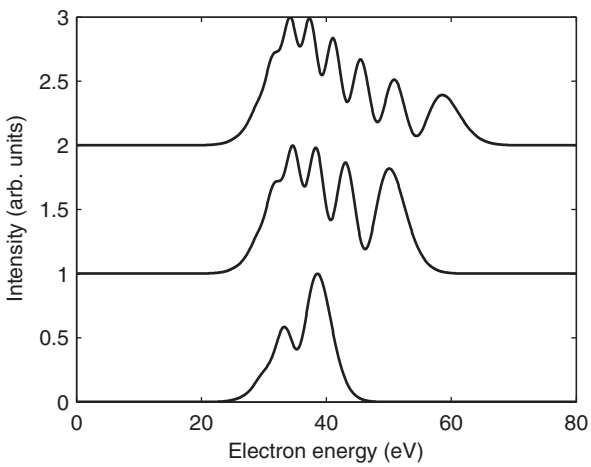

FIG. 1. The photoelectron spectra of H_2^+ excited by an XUV pulse from the ground state to the continuum states. The carrier frequency ω of the XUV laser pulse is 60 eV. The peak intensity of the XUV pulse is 1×10^{17}, 3×10^{17}, and 5×10^{17}, respectively, from the bottom curve to the top. The pulse width $\tau = 8 \times 2\pi/\omega = 0.547$ fs.

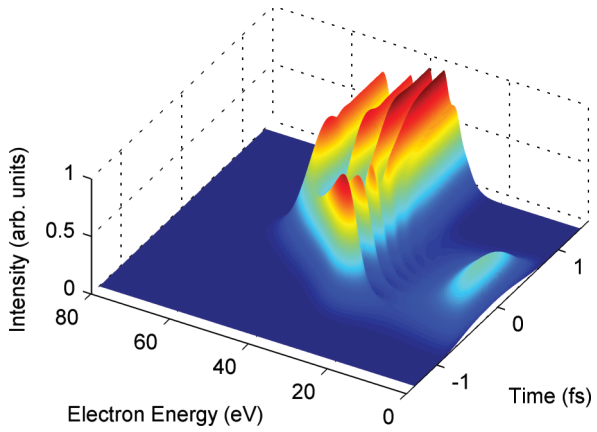

FIG. 2. (Color online) Dynamic development of the inference feature in the photoelectron spectrum. The simulation parameters are laser intensity $= 3 \times 10^{17}$ W/cm^2, laser pulse width $\tau = 8 \times 2\pi/\omega$, carrier frequency $\omega = 60$ eV. The time evolution of the photoelectron spectrum for H_2^+ is similar to that for a hydrogen atom (see Fig. 2 in Ref. [11]).

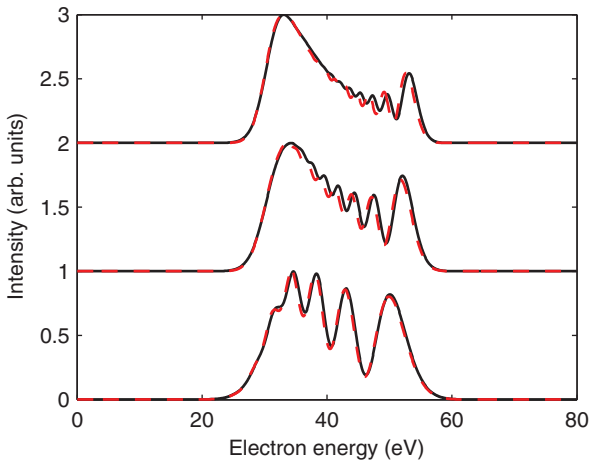

FIG. 3. (Color online) Dependence of the spectral interference fringes in the photoelectron spectra on the laser duration for an intensity of 3×10^{17} W/cm^2. The carrier frequency of the laser pulse is $\omega = 60$ eV. The pulse width is $\tau = 8 \times 2\pi/\omega$, $16 \times 2\pi/\omega$, and $24 \times 2\pi/\omega$, respectively, from the bottom to the top curve. The black solid curves are used for the computed results of H_2^+, while the red dashed curves are used for those of D_2^+.

laser intensity; and (iii) more interference fringes appear with increasing laser intensity.

For atomic hydrogen, pioneering work [11] has unveiled that the interference stems from the dynamic Stark effect, which is true for the photoelectron spectra of H_2^+ as well. It is known that the dynamic Stark effect induces an energy-level shift in proportion to the intensity of the laser pulses under certain conditions [30]. That is why the photoelectron spectrum becomes wider and manifests more interference fringes with increasing laser intensity.

To investigate the formation of the modulation structures in the photoelectron spectrum, we also illustrate the time evolution of the photoelectron spectrum in Fig. 2. Similar to Fig. 2 in Ref. [11], one can identify that the interference feature gradually appears and shifts to higher energy locations as the XUV laser pulse ascends, peaks, and descends in time, eventually forming the observed spectra with strong modulation shown in Fig. 1. The similarity of our result with that of a hydrogen atom [11] indicates that it is the dynamic Stark effect that accounts for the modulation structures in the photoelectron spectra.

The influence of the XUV laser pulse on the photoelectron spectrum for a hydrogen atom has been discussed in Ref. [18]. Here we also show the dependence of the photoelectron spectrum on the laser duration in Fig. 3. Two features are prominent in Fig. 3. First, the spectral width is almost constant. Second, the modulation fringes weaken monotonically to the high-energy end as the pulse duration is widened. The first point can be interpreted easily with the dynamic Stark effect. The maximum dynamic Stark energy shift depends only on the laser intensity, and thus the resultant photoelectron spectra under the same laser intensity exhibit almost the same widths.

The second point is interesting and promising in characterizing the details of the interference fringes. The physical picture presented for atomic hydrogen essentializes that the interference originates from two electronic waves which, dislodged at different times, are each exponentially weighted by a loss factor [11]. This energy-dependent factor is the integration of the laser-pulse envelope. The wider the laser pulse, the greater the difference between the two weighting factors. Therefore, the contrast ratio of the interference fringes becomes fainter. This explains why the modulation depth becomes gradually shallow as the laser pulse is widened, as illustrated in Fig. 3. The difference between the weighting factors is, however, smaller for higher energy electronic waves [11], and the interference is thus more discernible in the high-energy spectral portion. Meanwhile, it is recognizable that the interference fringes become denser and denser with increasing pulse width, which is reminiscent of the atomic hydrogen case, in which the phase accumulation for the interference is proportional to laser-pulse width.

Obviously it is harder to recognize the modulation structures in the photoelectron spectra for larger laser-pulse width, and so an ultrashort XUV laser pulse is required to verify this effect experimentally. The photoelectron spectra for D_2^+ are also overplotted in Fig. 3. The isotope D_2^+ shares the same dipole transition moment and PESs as those of H_2^+, while its reduced mass doubles as that of H_2^+, and so the slight difference in the photoelectron spectra for H_2^+ and D_2^+ implies that the nuclear motion has little influence on the interference spectral feature.

For the XUV laser pulses with the same peak intensity 3×10^{17} W/cm^2 but different durations $\tau = 8 \times 2\pi/\omega$, $16 \times 2\pi/\omega$, and $24 \times 2\pi/\omega$, the remaining or unionized portion $\int dR|\psi_g(R,+\infty)|^2 / \int dR|\psi_g(R,-\infty)|^2$ of H_2^+ is 0.36, 0.15, and 0.072, respectively. This means that a longer laser pulse shall lead to a higher ionization probability in general. We also find that it does not manifest a monotonic relationship between the remaining population and the laser intensity. Our findings are in accord with Fig. 6 in Ref. [26]. More importantly, the ionized population is large enough to detect the photoelectron spectra for the experimental verification.

In the discussion presented above, only qualitative analysis is made based on the dynamic Stark effect. It is the complexity

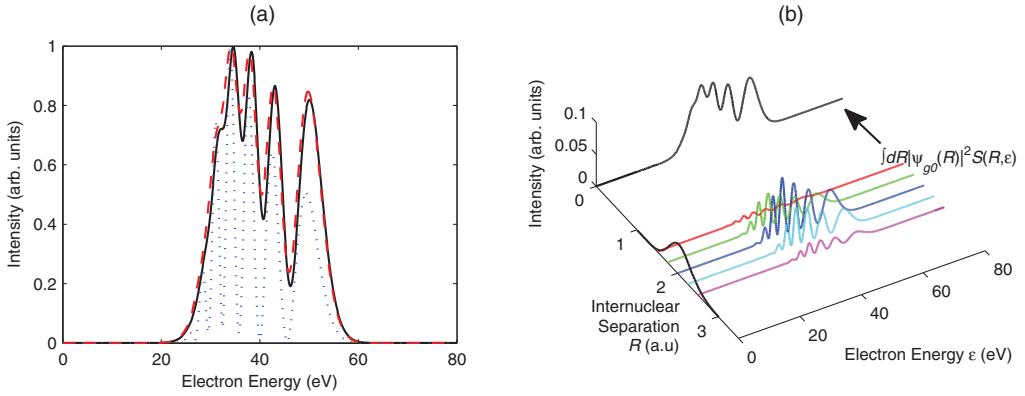

FIG. 4. (Color online) (a) Comparison of the photoelectron spectra computed by using our approximation (red dashed line) and that obtained without making the approximation (black solid line). The blue dotted line is for the photoelectron spectrum computed at the equilibrium internuclear separation. The simulation parameters are the same as those in Fig. 2. (b) Illustration of obtaining the total spectrum through the weighted summation of the photoelectron spectra computed at different internuclear separations under our approximation. The curve in the plane $R = 0$ is the total spectrum (multiplied by a proper constant number), and the curve in the plane $\varepsilon = 0$ is the weighting factor $|\psi_{g0}(R)|^2$. The colored curves are five typical partial photoelectron spectra, which are computed at different internuclear separations ($R = 1.5, 1.75, 2.0, 2.25,$ and 2.5 a.u.) and multiplied by their corresponding weighting factors.

of Eqs. (3) that prevents us from obtaining an analytical ansatz for the photoelectron spectrum. To gain deeper insight into the photoelectron spectra for the XUV laser-molecule interaction, we propose a fixed-nuclei approximation. Key to our approximation is neglecting the nuclear movement and considering the laser-molecule interaction process as a series (or an ensemble) of laser-atom interactions. In detail, for a fixed internuclear separation R, an electron of ionization potential $V_I(R) = [V_{\varepsilon=0}(R) - V_g(R)]$ is excited from the ground state to the continuum states, forming the photoelectron spectrum $S(R,\varepsilon)$. This spectrum $S(R,\varepsilon)$ can be computed through the numerical approach deployed in Refs. [11,18]. By interpreting the squared module of the nuclear ground-state wave function $|\psi_{g0}(R)|^2$ as the corresponding probability, we can express the total photoelectron spectrum $S_{\rm tot}(\varepsilon) = \int dR|\psi_{g0}(R)|^2 S(R,\varepsilon)$. Although we do not arrive at an explicit formula for the photoelectron spectrum, our approximation reflects the connection and disparity between the photoelectron spectra of an atom and a molecule. According to Ref. [11], the dynamic Stark energy shift of a hydrogen atom depends on the ionization potential. Therefore, the R dependence of the ionization potential implies that the dynamic Stark energy shift of $H_2{}^+$ is actually a function of the internuclear separation.

In Fig. 4(a) we compare the photoelectron spectrum computed by using our approximation with that obtained without making the approximation. It is obvious from Fig. 4(a) that the photoelectron spectrum obtained under our approximation reproduces nicely the spectrum calculated by solving Eqs. (3), which validates our approximation. We further examine the validity of our approximation by varying the laser intensity and pulse width, and the outcome suggests good robustness. A photoelectron spectrum $S(R_e)$ computed at the equilibrium internuclear separation is also presented in Fig. 4(a). It is found that the partial photoelectron spectrum computed at the equilibrium internuclear separation shares a similar profile with the total photoelectron spectrum but shows a stronger modulation feature than the total photoelectron spectrum. For the XUV laser-atom interaction, local approximation [31] and stationary-phase approximation [32] can be made to uncover the physical origin of the modulations in the photoelectron spectrum [11]. In our fixed-nuclei approximation, the photoelectron spectrum for the XUV laser-molecule interaction is a weighted superposition of that for the XUV laser-atom interaction. Due to the R dependence of the ionization potential, the superposition of the numerous different partial spectra may flatten the modulation structures, which makes the modulation in the total photoelectron spectrum weaker than that in the photoelectron spectrum computed at the equilibrium internuclear separation. The weighting factor $|\psi_{g0}(R)|^2$ maximizes at the equilibrium internuclear separation so that the resultant partial photoelectron spectrum resembles the total photoelectron spectrum.

In Fig. 4(b) we illustrate how the photoelectron spectra computed at different internuclear separations compose the total spectrum through the weighted summation. This picture implies that all the spectra generated by a weighted R-dependent atomic ensemble of different internuclear separations add up, yielding the overall spectral features. We are also convinced that our approximation can be applied to other molecules ionized by an intense XUV ultrashort pulse, as long as the single-photon process is dominant and the nuclear motion can be neglected during the laser pulse. It can be inferred from Fig. 4(b) that the interference photoelectron spectrum is jointly determined by the dipole transition moment and the PESs of the ground and excited states. All these observations await experimental confirmations.

IV. CONCLUDING REMARKS

In summary, by numerical simulation we find the modulation feature in the photoelectron spectra of molecular hydrogen ion $H_2{}^+$ ionized to the continuum states by an intense XUV laser pulse. For the hydrogen atom, the spectral modulation is unveiled to originate from the dynamic Stark effect, to which we similarly ascribe the modulation structures observed in

the photoelectron spectra of H_2^+. Our research reveals the impact of the laser parameters such as intensity and pulse width on the interference photoelectron spectra. On the basis of a pioneering physical picture for the hydrogen atom, we propose a fixed-nuclei approximation for molecules, which reproduces the spectrum precisely and reflects the relation and difference between the photoelectron spectra of an atom and a molecule. We anticipate that the modulated photoelectron spectra induced by sufficiently strong XUV laser pulses await more detailed investigation, together with the dynamic Stark effect counted on the nuclear degree of freedom.

ACKNOWLEDGMENT

The authors acknowledge support by the National Natural Science Foundation of China through Contract No. 10674100.

[1] W. Ackermann *et al*., Nat. Photon. **1**, 336 (2007).
[2] B. W. McNeil and N. R. Thompson, Nat. Photon. **4**, 814 (2010).
[3] M. Harmand *et al*., Nat. Photon. **7**, 215 (2013).
[4] C. Neidel, J. Klei, C.-H. Yang, A. Rouzée, M. J. J. Vrakking, K. Klünder, M. Miranda, C. L. Arnold, T. Fordell, A. L'Huillier, M. Gisselbrecht, P. Johnsson, M. P. Dinh, E. Suraud, P.-G. Reinhard, V. Despré, M. A. L. Marques, and F. Lépine, Phys. Rev. Lett. **111**, 033001 (2013).
[5] K. P. Singh, F. He, P. Ranitovic, W. Cao, S. De, D. Ray, S. Chen, U. Thumm, A. Becker, M. M. Murnane, H. C. Kapteyn, I. V. Litvinyuk, and C. L. Cocke, Phys. Rev. Lett. **104**, 023001 (2010).
[6] X. Wang, M. Chini, Y. Cheng, Y. Wu, X.-M. Tong, and Z. Chang, Phys. Rev. A **87**, 063413 (2013).
[7] S. H. Autler and C. H. Townes, Phys. Rev. **100**, 703 (1955).
[8] A. M. Bonch-Bruevich, N. N. Kostin, V. A. Khodovoĭ, and V.V. Khromov, Zh. Eksp. Teor. Fiz. **56**, 144 (1969) [Sov. Phys. JETP **29**, 82 (1969)].
[9] N. B. Delone and V. P. Krainov, Phys. Usp. **42**, 669 (1999).
[10] M. Chini, B. Zhao, H. Wang, Y. Cheng, S. X. Hu, and Z. Chang, Phys. Rev. Lett. **109**, 073601 (2012).
[11] P. V. Demekhin and L. S. Cederbaum, Phys. Rev. Lett. **108**, 253001 (2012).
[12] P. Balanarayan and N. Moiseyev, Phys. Rev. Lett. **110**, 253001 (2013).
[13] K. Toyota, O. I. Tolstikhin, T. Morishita, and S. Watanabe, Phys. Rev. A **76**, 043418 (2007).
[14] K. Toyota, O. I. Tolstikhin, T. Morishita, and S. Watanabe, Phys. Rev. A **78**, 033432 (2008).
[15] A. Brown, W. J. Meath, and P. Tran, Phys. Rev. A **63**, 013403 (2000).
[16] L. S. Cederbaum and W. Domcke, J. Phys. B **14**, 4665 (1981).
[17] W. Domcke, Phys. Rep. **208**, 97 (1991).
[18] C. Yu, N. Fu, G. Zhang, and J. Yao, Phys. Rev. A **87**, 043405 (2013).
[19] H. Yu, T. Zuo, and A. D. Bandrauk, Phys. Rev. A **54**, 3290 (1996).
[20] S. Chelkowski, C. Foisy, and A. D. Bandrauk, Phys. Rev. A **57**, 1176 (1998).
[21] M. Lein, T. Kreibich, E. K. U. Gross, and V. Engel, Phys. Rev. A **65**, 033403 (2002).
[22] B. M. Garraway and K. A. Suominen, Rep. Prog. Phys. **58**, 365 (1995).
[23] M. J. Holland, K.-A. Suominen, and K. Burnett, Phys. Rev. A **50**, 1513 (1994).
[24] M. Born and R. Oppenheimer, Ann. Phys. **389**, 457 (1927).
[25] B. T. Sutcliffe and R. G. Woolley, J. Chem. Phys. **137**, 22A544 (2012).
[26] P. V. Demekhin, Y.-C. Chiang, and L. S. Cederbaum, Phys. Rev. A **84**, 033417 (2011).
[27] F. Châteauneuf, T.-T. Nguyen-Dang, N. Ouellet, and O. Atabek, J. Chem. Phys. **108**, 3974 (1998).
[28] R. Kosloff and H. Tal-Ezer, Chem. Phys. Lett. **127**, 223 (1986).
[29] S.-M. Wang, K.-J. Yuan, Y.-Y. Niu, Y.-C. Han, and S.-L. Cong, Phys. Rev. A **74**, 043406 (2006).
[30] B. J. Sussman, Am. J. Phys. **79**, 477 (2011).
[31] See the Appendix in P. V. Demekhin and L. S. Cederbaum, Phys. Rev. A **83**, 023422 (2011).
[32] N. Bleinstein and R. Handelsman, *Asymptotic Expansions of Integrals* (Dover, New York, 1975).